Molecular quantum wakes for clearing fog

MALTE C. SCHROEDER,[1] ILIA LARKIN,[2] THOMAS PRODUIT,[1] ⓘ ERIC W. ROSENTHAL,[3] HOWARD MILCHBERG,[2] ⓘ AND JEAN-PIERRE WOLF[1,*]

[1]*Department of Applied Physics, University of Geneva, Chemin de Pinchat 22, 1211 Geneva 4, Switzerland*
[2]*Institute for Research in Electronics and Applied Physics, University of Maryland, College Park, MD 20742, USA*
[3]*U.S. Naval Research Laboratory, Washington, D.C. 20375, USA*
**Jean-Pierre.Wolf@unige.ch*

Abstract: High intensity laser filamentation in air has recently demonstrated that, through plasma generation and its associated shockwave, fog can be cleared around the beam, leaving an optically transparent path to transmit light. However, for practical applications like free-space optical communication (FSO), channels of multi-centimeter diameters over kilometer ranges are required, which is extremely challenging for a plasma based method. Here we report a radically different approach, based on quantum control. We demonstrate that fog clearing can also be achieved by producing molecular quantum wakes in air, and that neither plasma generation nor filamentation are required. The effect is clearly associated with the rephasing time of the rotational wave packet in N_2. Pump excitation provided in the form of resonant trains of 8 pulses separated by the revival time are able to transmit optical data through fog with initial extinction as much as -6 dB.

1. Introduction

Light scattering by small particles is a key issue for several optical applications, such as imaging through turbid media or free space optical telecommunication (FSO) between ground based stations and satellites. Many approaches based on adaptive optics and spatio-temporal shaping of laser beams have been proposed for improving the propagation through scattering media and for avoiding speckle patterns formation [1–6]. These methods, however, are of limited use for dense and extended structures such as atmospheric fog and clouds. For free space optical networks, this critical issue is currently mitigated by the multiplication of transmitting/receiving stations, which increases complexity and cost. Until recently no active method for opening clear optical transmission channels through clouds or fog was available. The propagation of ultrashort and high intensity lasers through the atmosphere provided a radically new concept, based on plasma generation inherent to laser filamentation [7–9]. Laser filaments are self-sustained light structures with a typical core diameter $d_{core} \sim 100 \, \mu m$ (at 800 nm) and up to hundreds of meters in length, orders of magnitude beyond the linear diffraction limit. They stem from the dynamic balance between self-focusing (Kerr effect) and defocusing (diffraction, plasma-induced refraction, etc.) that takes place during non-linear laser propagation in air [10]. Filaments bear high intensities ($10 - 100 \, TW/cm^2$) and generate a low density plasma during propagation. The plasma recombination thermalizes quickly, resulting in a very rapid local increase of pressure that drives a single cycle cylindrical acoustic wave [11–15]. Over a time window of $0.1 - 1$ ms, this leads to a reduced air density channel significantly wider than the filament core [13–17]. When launched in fog (water droplet diameter centered around $5 \, \mu m$), this filament-induced shockwave radially ejects the scatterers out of the beam [8,9]. This fog clearing mechanism requires modest energy deposition, of the order of less than 1 mJ/m [18,19]. For droplets densities $N_d \sim 10^5 \, cm^{-3}$, it was shown that the filament formation is not significantly altered [20]. This is the case in the

vast majority of scenarios in the field [20–22], and is the case for our fog chamber as discussed below. Under these conditions, there is little additional energy cost due to this droplet clearing mechanism, as the energy deposition and acoustic wave generation through plasma generation by the filament occurs in any case as a consequence of its propagation.

However, applying the filament-induced clearing method to real-scale FSO may be challenging. Opened communication channels require lengths of at least several hundred meters and diameters of ∼ 10 cm. Laboratory scale experiments demonstrated that filament-induced acoustic waves could clear regions exceeding the filament dimensions, but not larger than 0.5 − 1 cm [9]. Engineering the laser pulse properties (adaptive optics and temporal focusing) in order to achieve uniform filament excitation over several hundred meters appears particularly challenging.

In the present paper, we generate and coherently control rotational wave packets in the air molecules (in particular N_2) to produce an acoustic wave to open transmission channels in fog and clouds over short distances without requiring plasma formation or filamentation. Larger diameter beams and/or mid-IR lasers could then be used for fog clearing, which when filamenting generate lower density plasma unsuited for shockwave creation, but for which long distance propagation is more easily achievable and controllable [23,24].

2. Coherent control of rotational wave packets in air molecules

The effects of laser induced molecular alignment and field-free coherent rotation on laser propagation have been investigated by several authors [25–29]. Impulsive Raman scattering induces a coherent superposition of rotational states $|J, m\rangle$ in N_2 and O_2, i.e. rotational wave packets

$$|\Psi_R(t)\rangle = \sum_{J,m} c_{J,m}|J, m\rangle e^{-iE_R t/\hbar}, \tag{1}$$

where J and m are the quantum numbers of the total and z-component of the rotational angular momentum and $E_R = hcBJ(J + 1)$ the rotational state energies of the rigid rotor Hamiltonian (with B the rotational constant, h the Planck constant and c the speed of light). The instantaneous non-adiabatic laser excitation locks in phase all the Raman-excited rotational states at $t = 0$, and the resulting wave packet evolves as in Eq. (1). For $t>0$, the states in the sum dephase with respect to each other and the wave packet spreads. However, rephasing occurs in the form of revivals at specific times, leading to full re-alignment at periodic intervals of $\Delta t = T_R = 1/2Bc$ (8.36 ps in N_2 and 11.2 ps in O_2). These effects have been measured using Coulomb explosion imaging in very low density gases [30] and, importantly for laser propagation applications, the effects persist at atmospheric pressure [29,31]. Due to the even integer distribution of the rotational frequencies, additional alignment or anti-alignment recurrences also occur at $t = T_R/4$, $t = T_R/2$, and $t = 3T_R/4$ [30,31].

The periodic field-free alignment takes place until decoherence occurs, due to inter-molecular collisions and/or centrifugal distortion (deviation from the rigid rotor Hamiltonian). Typical rotational coherence times observed in N_2 at standard temperature and pressure are ∼ 80 ps [33]. Within this coherence time window, the rotational quantum wake can be coherently controlled by a train of short pulses precisely separated by the full revival time T_R, matching the «quantum echoes» of the rotating molecule, as demonstrated by Cryan et al [33]. This coherent control method based on repetitive impulsive Raman excitation was originally proposed by Weiner et al [34] for controlling phonons in organic solids. By shaping the laser excitation as a sequence of 4 pulses separated by T_R, Zahedpour et al [29] recently demonstrated that the molecular rotation of N_2 was driven to equivalent temperatures as high as 450 K (30 meV/molecule of additional heating). Conversely, rotation was coherently hindered by applying series of pulses resonant at times for which molecules are anti-aligned ($T_R/2$). Collisional decoherence and thermalization of the rotationally excited molecules after ∼ 100 ps [13] generates an on-axis pressure spike that drives a single-cycle acoustic wave. The amplitude of this wave was shown to

exceed that previously observed in plasma filaments [29]. In the present paper, we demonstrate that this plasma-free acoustic wave can also efficiently eject water droplets out of the beam, and that the coherently controlled quantum wake creates clear channels in fog without the need for filamentation-based ionization.

3. Experiment

For the experimental demonstration of the concept, we used a train of 8 ultrashort pulses, which provides an optimal compromise between the number of successive Raman excitations and the onset of decoherence due to collisions and centrifugal distortion.

A sketch of the experimental set-up is shown in Fig. 1. The laser pump consists of either a single pulse or a train of eight $\lambda = 800$ nm, 56 fs Ti:Sapphire (TiSa) pulses produced with a Michelson interferometer [32] («pulse stacker»). The beam is focused with an f/80 lens into the fog chamber. The FWHM of the vacuum beam waist is about $w_{FWHM} = 25$ μm and the femtosecond laser train is repeated at a frequency of 1 kHz. The energy per pulse in the train is 0.48 mJ. A continuous wave (CW) counter-propagating laser at $\lambda = 1.55$ μm, spatially overlapping the TiSa beam, is used for measuring changes in transmission through the fog, and for investigating the dynamics of the droplets expulsion by the acoustic wave. In addition, a 10 Hz frequency doubled Nd:YAG laser ($\lambda = 532$ nm) is synchronized to the TiSa pump beam to probe the 2D gas density at variable delays by shadowgraphy and interferometry.
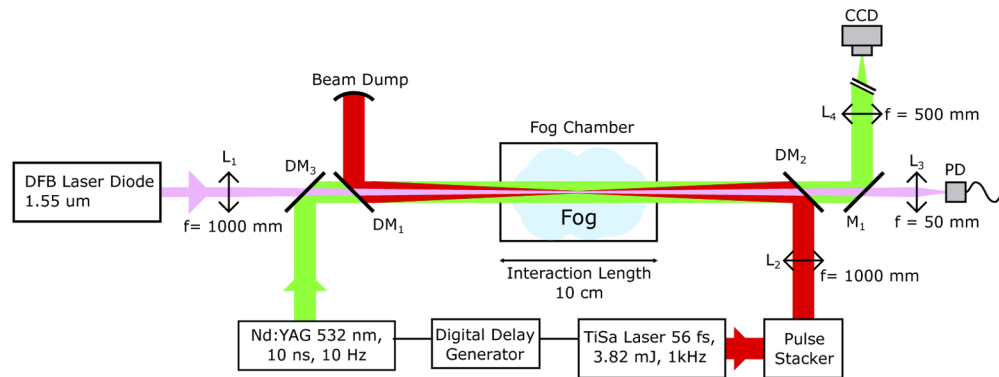

Fig. 1. Quantum wake clearing of fog: a series of 8 pulses of 56 fs are generated by a nested Michelson interferometer (pulse stacker [32]) and softly focused into a fog chamber. The interval between the pulses can be tuned on- or off-resonance with the rotational revival times T_R of the nitrogen molecules in air. Clearing of the fog is assessed with a counter-propagating CW laser at telecom wavelength (1.55 μm) and a photodiode that measures the transmission. In addition a synchronized Nd:YAG laser is used for imaging the induced shockwave by shadowgraphy and interferometry

In order to simulate realistic fog/cloud conditions, the size distribution of the droplets in the cloud chamber is centered on a radius of 5 μm (measured by a Grimm 1.109 particle sizer). The droplet number density is variable from 0 to 1.5×10^5 cm^{-3} (1000 times more than in a cumulus cloud) [9]. This variation in N_d corresponds to attenuation ranging from 0 dB (no fog) to -10 dB. The droplets were generated and dispersed by a piezo-driven ultrasonic source.

The shadowgraphic measurements allow for the observation of changes in the atmospheric pressure caused by the acoustic wave produced by the resonantly and off-resonantly spaced pulse trains. The shadowgraphic image in Fig. 2(b) shows the acoustic wave produced in fog (droplet concentration 1.3×10^5 cm^{-3}) when the pump laser consists of a train of 8 pulses of 56 fs duration, separated by 8.36 ps, i.e. resonant with the full rephasing time of the rotational wave packet.

Each of the 8 pulses bears an intensity of the order of $\sim 10^{13}$ W/cm^2 at the beam waist. A clear radially expanding wave is produced, which reduces the air density in the center of the beam (typ. $500 - 700\,\mu$m diameter) during the first hundred μs after the pulse train. The reduced density region exhibits a lower refractive index (Fig. 3(b)), which induces defocusing of the Nd:YAG probe laser, and thus a loss in the transmitted light. The depleted density region is eventually refilled by the surrounding gas after a few hundreds microseconds, as shown in the supplementary videos **Visualization 1** and **Visualization 2**. The acoustic wave expansion characteristics, in terms of amplitude and speed, appear almost unaffected by the presence of droplets, similar to previously reported measurements in clean air [12]. Conversely, if the time separation between the pulses within the train is slightly detuned away from resonance (8.66 ps), a much weaker shockwave is produced (Fig. 2(a)), revealing a smaller temperature rise and refractive index shift in the gas (Fig. 3(a)). These results demonstrate that the dominant mechanism responsible for the acoustic wave production here is the coherent control of the molecular quantum wake and not plasma generation (also confirmed by single pulse measurements, Fig. 5).
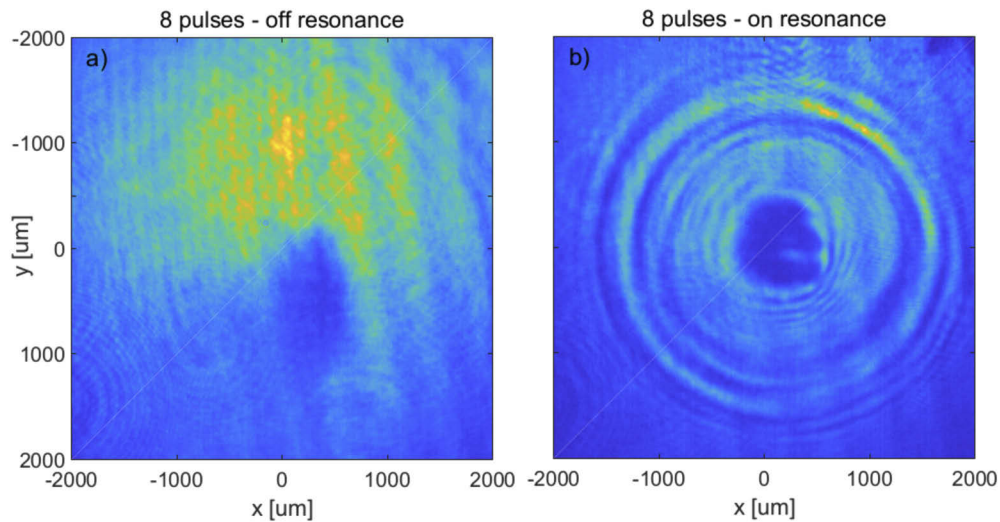

Fig. 2. Coherent control of the rotational quantum wake induced shockwave in fog. Visualized through shadowgraphic measurements. Left: train with pulse intervals slightly detuned from resonance: 8.66 ps; Right: train of 8 pulses tuned in resonance with the full revival time for N$_2$: 8.36 ps . Delay between TiSa pump and Nd:YAG probe: 4 μs. Total energy of the pump pulse train: 3.8 mJ

A folded wavefront interferometer was insterted upstream of the imaging apparatus to measure the refractive index shift in the reduced density region surrounding the beam center. Gas density was extracted from retrieved interferograms using well-established fringe analysis techniques [35]. For these measurements no fog was added to the chamber, as to prevent turbulence in the fog from interfering with the acquisition of the interferograms. Figure 3(a) shows the variation of the refractive index for the off-resonant case, where the pulses in the train are detuned by 300 fs relative to each other, at a pump-probe delay of 500 μs. The reduced density region is visible at the prior location of the beam center, gradually expanding outward from this point. At the center, the relative refractive index shift is $\Delta n_{off} \approx -7.8 \times 10^{-6}$. If the pulse train is tuned to the revival time of molecular nitrogen, the reduced density region increases significantly in size and depth. At the same time delay of 500 μs, the resulting refractive index shift increases approximately by a factor of 2 to $\Delta n_{on} \approx -16.2 \times 10^{-6}$ (Fig. 3(b)). The asymmetry visible in the figure stems from convection [28]. In the insets the filling in of the reduced density region can be observed
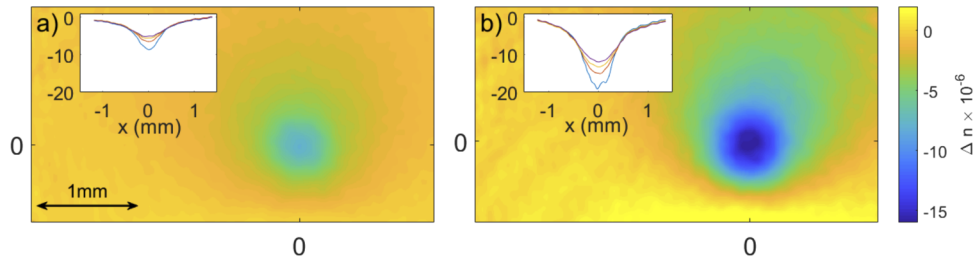
Fig. 3. Change in air refractive index due to rotational gas heating, measured by interferometry. Left: detuned pulse train: 8.66 ps; Right: resonant pulse train at full revival time for N_2: 8.36 ps . Delay between TiSa pump and Nd:YAG probe: 500 μs. The insets show the shift in the refractive index for time delays of 200, 400, 600 and 800 μs after the pump, in order of deepest to shallowest.

by the smoothing of the lineouts over time. The lineouts depict the spatially resolved change in refractive index along the x-axis, centered on the minimum value at the core.

These observations are consistent with the shadowgraphy measurements. The more efficient rotational molecular gas heating in the resonant case results in more heat deposition in the air. Consequently, the higher temperature gradient causes a stronger acoustic wave, which more efficiently reduces the air density over a more extended region.

The gain in transmission provided by the quantum wake clearing process was assessed by running the probe telecom laser in a CW mode (Fig. 4). Figure 4(a) shows the effect of the 8-pulse train pump on the transmission of the $\lambda = 1.55\,\mu$m CW laser in the absence of fog. The air density depletion due to rotational heating causes an initial defocusing of the telecom laser due to the induced refractive index gradient. This leads to the observed modulation of the signal at 1 kHz, due to the finite aperture of the detection system. In this geometry, the envelope of the modulation requires $2-3$ ms to reach a steady state. In the presence of fog ($N_d \sim 1.3\times 10^5$ cm^{-3}), corresponding to 9 dB attenuation, the 8-pulse train dramatically increases the telecom laser transmission by a factor 3 (i.e. 4.8 dB) when the pulse interval in the train is tuned on-resonance with the full revival time of 8.36 ps (Fig. 4(b)). Interestingly, the modulated envelope reaches a steady state after $\sim 7-8$ ms, longer than in the droplet-free case. This can be interpreted by the fact that the first few 8-pulse trains, delivered at 1 kHz, are used to clear the initial local droplet concentration to make its way for the following pulses. Conversely, when the 8-pulse interval is tuned slightly off-resonance, the gain drops to a factor of only ~ 1.5 (1.7 dB, Fig. 4(c)). This remaining gain is caused by partial rotational heating.

The efficiency of rotational heating-induced fog clearing was assessed as a function of the fog's optical density, by varying the droplet number density in the chamber. Although large fluctuations are present due to instabilities in the cloud chamber (entrance and exits are open to the ambient air), a clear enhancement in transmission is observed for all the optical density values in the case of the on-resonance pump pulse trains. As quantitative assessment of the process efficiency, we consider the maximum initial cloud extinction value for which transmission is fully recovered (100%, i.e. 0 dB extinction). For the on-resonance pulse train, this value corresponds to -6 dB initial extinction, while for the slightly detuned pulse train, it drops to -2 dB. It is now relevant to compare these values to the values achieved with a single pulse (Fig. 5(b) (with all other experimental conditions kept identical to the 8 pulses train case). When only one pulse of the train is used (bearing 0.48 mJ as in the pulse train), no transmission gain is observed, which suggests that the plasma generation of individual pulses of the train is negligible. Conversely if the whole energy of the pulse train, 3.8 mJ, is concentrated in a single pulse, plasma generation and filamentation are initiated, and we observe the associated acoustic wave clearing process seen
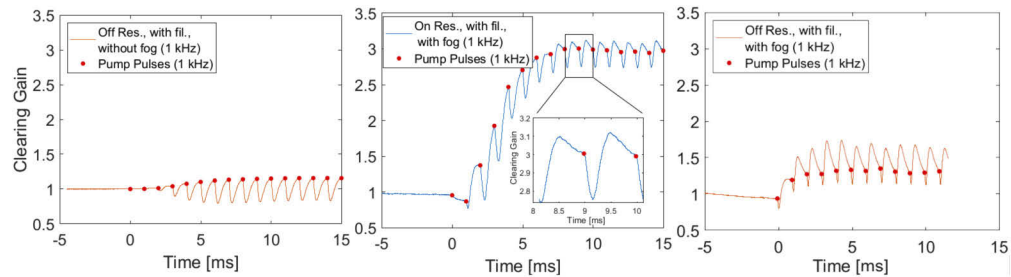
Fig. 4. Fog clearing induced by the rotational quantum wake. Transmission gain in the case of (a) No fog with the 8 pulse train pump laser, (b) Fog (1.3×10^5 cm^{-3} droplet concentration) with the 8 pulse train tuned on-resonance with the quantum wake rephasing time, and (c) Fog (0.7×10^5 cm^{-3} droplet concentration) with the 8 pulse train tuned off-resonance with the quantum wake rephasing time. Total energy of the pump: 3.8 mJ. Transmission is normalized to 1 in each case, corresponding to the situation where no pump is present ($t<0$).

previously [8,9], i.e. -8 dB, which exceeds the quantum wake clearing process with 8 pulses. Also, the slope significantly exceeds the slope in the case of rotational heating with the pulse train. The linear increase in the transmission gain was previously attributed [8] to the fact that the number of droplets ΔN ejected by the shockwave is proportional to the number of droplets N initially present in the volume (percentage of droplets cleared in the channel: on resonance: 57.4%; off resonant: 28.0% ; 1 pulse full energy : 75.1% ; 1 pulse 1/8th of energy: 0%). In other words, the energy of the shockwave is not significantly altered by the quantity of droplets that have to be moved.
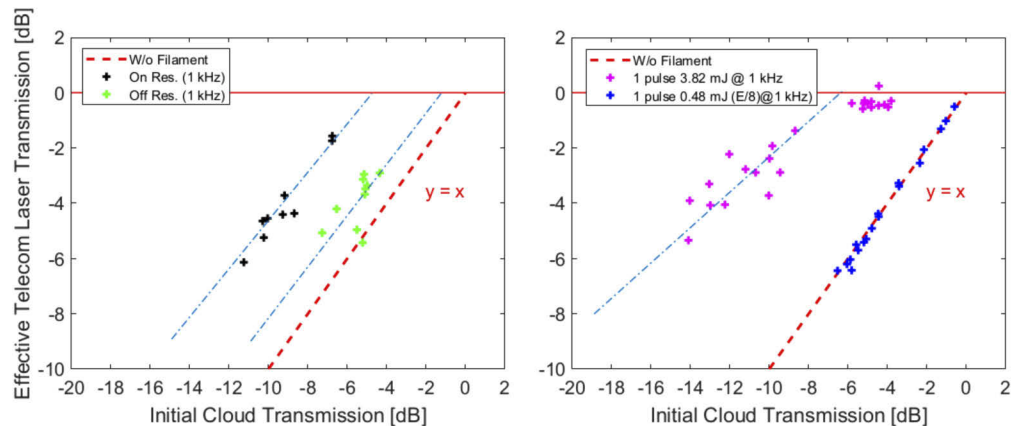

Fig. 5. Fog clearing induced by the rotational quantum wake as a function of the initial signal attenuation caused by different fog densities 5(a). Clearing is efficient for all densities in the case of a pulse train in resonance with the rephasing time, and the efficiency increases with the initial density (see text). Clearing is strongly reduced for the off-resonant case. 5(b) comparison with the plasma induced shockwave - Purple: single pulse of 3.8 mJ (entire energy of the train in one pulse), Blue : single pulse of 0.48 mJ (one pulse of the train). Transmission is normalized to 1 in each case, corresponding to the situation where no pump is present ($t<0$).

As already mentioned above, the clear enhancement of the transmission at the rephasing time of the N_2 rotational wave packet, as compared to the non-resonant case, excludes dominant clearing processes like droplet explosion, shattering or direct evaporation by the laser beam.

However, in the present configuration, the rotational heating of the gas itself (450 K) exceeds the vaporization temperature of water, so that the partial or complete evaporation of the droplets by heat transfer from the hot air to the droplets may have a contribution in the fog clearing as well. Although the exact calculation of the transient evaporated mass rate from a moving droplet is a complex problem [36], some qualitative arguments can be drawn for assessing this role in the clearing. A necessary (but not sufficient) condition for the process to occur is that the amount of energy Q required for vaporizing the ensemble of droplets in the channel is less than or equal to the energy deposited by the laser. With $1.5 \times 10^5 \, \text{cm}^{-3}$ droplets in a channel of 0.5 mm radius and 10 cm length, this leads to $Q = 13$ mJ, which means that all the incoming laser energy should be deposited in the gas and then transferred from the heated gas to the droplets with an efficiency of 100%. These considerations suggest that the droplet vaporization by the heated gas does not play the major role in the fog clearing process, in contrast to the displacement of the drops by the acoustic wave as previously observed for the filament induced clearing process [8,9,37].

4. Conclusion

In this article, we demonstrated that neither ionization nor filamentation are required to produce a fog clearing acoustic wave, as they can be substituted by quantum controlled rotational heating in air. This discovery opens new perspectives in the application of the method for real, atmospheric scale operation like FSO. For instance, intense mid-IR lasers, which provide only moderate ionization as they propagate in air [38–41], are now potentially very attractive candidates for fog clearing applications. It was recently reported in particular that TW peak powers CO_2 lasers can provide wide diameter self-guiding channels over kilometric distances [24], fulfilling the requirements for FSO between earth and satellites.

Disclosures

The authors declare no conflicts of interest.

References

1. O. Katz, E. Small, Y. Bromberg, and Y. Silberberg, "Focusing and compression of ultrashort pulses through scattering media," Nat. Photonics **5**(6), 372–377 (2011).
2. A. P. Mosk, A. Lagendijk, G. Lerosey, and M. Fink, "Controlling waves in space and time for imaging and focusing in complex media," Nat. Photonics **6**(5), 283–292 (2012).
3. O. Katz, P. Heidmann, M. Fink, and S. Gigan, "Non-invasive single-shot imaging through scattering layers and around corners via speckle correlations," Nat. Photonics **8**(10), 784–790 (2014).

4. D. J. McCabe, A. Tajalli, D. R. Austin, P. Bondareff, I. A. Walmsley, S. Gigan, and B. Chatel, "Spatio-temporal focusing of an ultrafast pulse through a multiply scattering medium," Nat. Commun. **2**(1), 447 (2011).

5. I. M. Vellekoop and A. P. Mosk, "Focusing coherent light through opaque strongly scattering media," Opt. Lett. **32**(16), 2309 (2007).

6. A. Boniface, M. Mounaix, B. Blochet, R. Piestun, and S. Gigan, "Transmission-matrix-based point-spread-function engineering through a complex medium," Optica **4**(1), 54–59 (2017).

7. L. Bergé, S. Skupin, R. Nuter, J. Kasparian, and J. P. Wolf, "Ultrashort filaments of light in weakly ionized, optically transparent media," Rep. Prog. Phys. **70**(10), 1633–1713 (2007).

8. G. Schimmel, T. Produit, D. Mongin, J. Kasparian, and J.-P. Wolf, "Free space laser telecommunication through fog," Optica **5**(10), 1338 (2018).

9. L. De La Cruz, E. Schubert, D. Mongin, S. Klingebiel, M. Schultze, T. Metzger, K. Michel, J. Kasparian, and J. P. Wolf, "High repetition rate ultrashort laser cuts a path through fog," Appl. Phys. Lett. **109**(25), 251105 (2016).

10. A. Couairon and L. Bergé, "Light Filaments in Air for Ultraviolet and Infrared Wavelengths," Phys. Rev. Lett. **88**(13), 135003 (2002).

11. N. Jhajj, E. W. Rosenthal, R. Birnbaum, J. K. Wahlstrand, and H. M. Milchberg, "Demonstration of long-lived high power optical waveguides in air," Phys. Rev. X **4**(1), 011027 (2014).

12. J. K. Wahlstrand, N. Jhajj, E. W. Rosenthal, S. Zahedpour, and H. M. Milchberg, "Direct imaging of the acoustic waves generated by femtosecond filaments in air," Opt. Lett. **39**(5), 1290 (2014).

13. Y. H. Cheng, J. K. Wahlstrand, N. Jhajj, and H. M. Milchberg, "The effect of long timescale gas dynamics on femtosecond filamentation," Opt. Express **21**(4), 4740 (2013).

14. O. Lahav, L. Levi, I. Orr, R. A. Nemirovsky, J. Nemirovsky, I. Kaminer, M. Segev, and O. Cohen, "Long-lived waveguides and sound-wave generation by laser filamentation," Phys. Rev. A **90**(2), 021801 (2014).

15. G. Point, C. Milián, A. Couairon, A. Mysyrowicz, and A. Houard, "Generation of long-lived underdense channels using femtosecond filamentation in air," J. Phys. B: At., Mol. Opt. Phys. **48**(9), 094009 (2015).

16. F. Vidal, D. Comtois, C. Y. Chien, A. Desparois, B. L. Fontaine, T. W. Johnston, J. C. Kieffer, H. P. Mercure, H. Peépin, and F. A. Rizk, "Modeling the triggering of streamers in air by ultrashort laser pulses," IEEE Trans. Plasma Sci. **28**(2), 418–433 (2000).

17. J. Yu, D. Mondelain, J. Kasparian, E. Salmon, S. Geffroy, C. Favre, V. Boutou, and J.-P. Wolf, "Sonographic probing of laser filaments in air," Appl. Opt. **42**(36), 7117–7120 (2003).

18. E. W. Rosenthal, N. Jhajj, I. Larkin, S. Zahedpour, J. K. Wahlstrand, and H. M. Milchberg, "Energy deposition of single femtosecond filaments in the atmosphere," Opt. Lett. **43**(3), 366 (2018).

19. A. Houard, V. Jukna, G. Point, Y.-B. André, S. Klingebiel, M. Schultze, K. Michel, T. Metzger, and A. Mysyrowicz, "Study of filamentation with a high power high repetition rate ps laser at 1.03 μm," Opt. Express **24**(7), 7437 (2016).

20. F. Courvoisier, V. Boutou, J. Kasparian, E. Salmon, G. Méjean, J. Yu, and J. P. Wolf, "Ultraintense light filaments transmitted through clouds," Appl. Phys. Lett. **83**(2), 213–215 (2003).

21. S. Skupin, L. Bergé, U. Peschel, and F. Lederer, "Interaction of femtosecond light filaments with obscurants in aerosols," Phys. Rev. Lett. **93**(2), 023901 (2004).

22. M. Kolesik and J. V. Moloney, "Self-healing femtosecond light filaments," Opt. Lett. **29**(6), 590 (2004).

23. P. Panagiotopoulos, P. Whalen, M. Kolesik, and J. V. Moloney, "Super high power mid-infrared femtosecond light bullet," Nat. Photonics **9**(8), 543–548 (2015).

24. S. Tochitsky, E. Welch, M. Polyanskiy, I. Pogorelsky, P. Panagiotopoulos, M. Kolesik, E. M. Wright, S. W. Koch, J. V. Moloney, J. Pigeon, and C. Joshi, "Megafilament in air formed by self-guided terawatt long-wavelength infrared laser," Nat. Photonics **13**(1), 41–46 (2019).

25. F. Calegari, C. Vozzi, S. Gasilov, E. Benedetti, G. Sansone, M. Nisoli, S. De Silvestri, and S. Stagira, "Rotational Raman effects in the wake of optical filamentation," Phys. Rev. Lett. **100**(12), 123006 (2008).

26. M. Renard, E. Hertz, S. Gurin, H. R. Jauslin, B. Lavorel, and O. Faucher, "Control of field-free molecular alignment by phase-shaped laser pulses," Phys. Rev. A **72**(2), 025401 (2005).

27. S. Varma, Y. H. Chen, J. P. Palastro, A. B. Fallahkair, E. W. Rosenthal, T. Antonsen, and H. M. Milchberg, "Molecular quantum wake-induced pulse shaping and extension of femtosecond air filaments," Phys. Rev. A **86**(2), 023850 (2012).

28. N. Jhajj, Y.-H. Cheng, J. K. Wahlstrand, and H. M. Milchberg, "Optical beam dynamics in a gas repetitively heated by femtosecond filaments," Opt. Express **21**(23), 28980 (2013).

29. S. Zahedpour, J. Wahlstrand, and H. Milchberg, "Quantum Control of Molecular Gas Hydrodynamics," Phys. Rev. Lett. **112**(14), 143601 (2014).

30. J. Huang, C. Wu, N. Xu, Q. Liang, Z. Wu, H. Yang, and Q. Gong, "Field-induced alignment of oxygen and nitrogen by intense femtosecond laser pulses," J. Phys. Chem. A **110**(34), 10179–10184 (2006).

31. Y.-H. Chen, S. Varma, A. York, and H. M. Milchberg, "Single-shot, space- and time-resolved measurement of rotational wavepacket revivals in H2, D2, N2, O2, and N2O," Opt. Express **15**(18), 11341–11357 (2007).

32. C. W. Siders, J. L. W. Siders, A. J. Taylor, S.-G. Park, and A. M. Weiner, "Efficient high-energy pulse-train generation using a 2^n -pulse michelson interferometer," Appl. Opt. **37**(22), 5302–5305 (1998).

33. J. P. Cryan, P. H. Bucksbaum, and R. N. Coffee, "Field-free alignment in repetitively kicked nitrogen gas," Phys. Rev. A **80**(6), 063412 (2009).

34. A. M. Weiner, D. E. Leaird, G. P. Wiederrecht, and K. A. Nelson, "Femtosecond Pulse Sequences Used for Optical Manipulation of Molecular Motion," Science **247**(4948), 1317–1319 (1990).
35. M. Takeda, H. Ina, and S. Kobayashi, "Fourier-transform method of fringe-pattern analysis for computer-based topography and interferometry," J. Opt. Soc. Am. **72**(1), 156–160 (1982).
36. W. A. Sirignano, *Fluid dynamics and transport of droplets and sprays, second edition* (Cambridge University Press, Irving, 2010), 2nd ed.
37. J. P. Wolf, "Short-pulse lasers for weather control," Rep. Prog. Phys. **81**(2), 026001 (2018).
38. D. Mongin, V. Shumakova, S.Ališauskas, E. Schubert, A. Pugžlys, J. Kasparian, J. P. Wolf, and A. Baltuška, "Conductivity and discharge guiding properties of mid-IR laser filaments," Appl. Phys. B: Lasers Opt. **122**(10), 267 (2016).
39. A. V. Mitrofanov, A. A. Voronin, D. A. Sidorov-Biryukov, A. Pugžlys, E. A. Stepanov, G. Andriukaitis, T. Flöry, S.Ališauskas, A. B. Fedotov, A. Baltuška, and A. M. Zheltikov, "Mid-infrared laser filaments in the atmosphere," Sci. Rep. **5**(1), 8368 (2015).
40. H. Liang, D. L. Weerawarne, P. Krogen, R. I. Grynko, C.-J. Lai, B. Shim, F. X. Kärtner, and K.-H. Hong, "Mid-infrared laser filaments in air at a kilohertz repetition rate," Optica **3**(7), 678 (2016).
41. D. Kartashov, S.Ališauskas, A. Pugžlys, A. Voronin, A. Zheltikov, M. Petrarca, P. Béjot, J. Kasparian, J.-P. Wolf, and A. Baltuška, "Mid-infrared laser filamentation in molecular gases," Opt. Lett. **38**(16), 3194 (2013).